JOURNAL OF MATERIALS SCIENCE 19 (1984) 1767–1776

Electrical conductivity of single crystal and polycrystalline yttria-stabilized zirconia

S. P. S. BADWAL
CSIRO, Division of Materials Science, Advanced Materials Laboratory, P.O. Box 4331, Melbourne, Victoria, Australia 3001

The conductivity of several single crystal and polycrystalline Y_2O_3–ZrO_2 samples has been studied by complex impedance and four-probe direct current techniques. For single crystals only one arc, due to lattice conductivity, was observed in the complex impedance representation. Polycrystalline materials showed a second arc, due to grain boundary resistance, the extent of which decreased as the impurity concentration was reduced and as the electrolyte microstructure improved. The activation energies for the volume and total conductivity of the purest polycrystalline samples were similar and agreed with those for the single crystals. These values, however, decreased by 20 to 25 kJ mol^{-1} on going from low ($< 550°$ C) to high ($> 850°$ C) temperatures. The change in the activation energy with temperature is thought to be due to a gradual transition between an association region, where vacancies are bound to dopant cations, and a dissociation region where vacancies are free and mobile.

1. Introduction

Yttria-stabilized zirconia is known to be an anionic conductor over wide ranges of temperature and oxygen partial pressure. It is commonly used in the polycrystalline form as an electrolyte in electrochemical devices such as oxygen pumps, sensors, fuel cells and steam electrolysers [1–3]. These materials often contain poorly conducting impurities (e.g. SiO_2, Al_2O_3) as sintering aids. Alternatively, impurities can be incorporated as contamination during preparation and handling. These impurities tend to decrease the conductivity by dissolving in the grains of the conducting phase and/or by segregating at the grain boundaries [4, 5]. Segregation may be associated with the formation of new boundary phases. In the absence of these poorly conducting phases, the conductivity is influenced by the dopant level, grain size, porosity, the constriction of current lines and, at low temperatures, by dopant cation–vacancy interactions [5, 6]. Arrhenius plots of the conductivity consistently show a change in the slope towards a higher activation energy at low temperatures [7, 8]. Both grain boundary resistance and dopant cation–vacancy interactions dominate increasingly at low temperatures and thus can influence the shape of these plots.

Grain boundary resistance is often higher for poorly defined (microinhomogeneous) electrolyte microstructures; it increases with impurity level [9, 10] and porosity [11] and decreases with increase in the grain size [12, 13]. Thus for high density, pure polycrystalline materials with well prepared microstructures the contribution from the grain boundary resistance should be relatively small and for single crystals free of microinhomogeneities it should disappear completely [14, 15].

The present work is mainly devoted to studying the effects of minor impurities and preparation techniques on the grain-boundary resistance and their influence on the low temperature conductivity behaviour. In addition we have made measurements on single crystals of Y_2O_3–ZrO_2 in order to determine whether grain boundary effects contribute to the change in the slope of the Arrhenius plots below about 600° C, and whether the slope change is indeed real [5, 7, 8, 15] or an artefact of the experimental technique [16].

0022–2461/84 $03.00 + .12

TABLE I Details of specimen preparation and densities

Series	Electrolyte composition	Method of preparation	Heat treatment, T°C (h)	Measured density % of theoretical
A	8.7 mol % Y_2O_3 + 91.3 mol % ZrO_2	*	–	–
B†	10.1 mol % Y_2O_3 + 89.9 mol % ZrO_2	coprecipitation	1900 (4)	94
C‡	10 mol % Y_2O_3 + 90 mol % ZrO_2	mixed oxide	1700 (15)	
			1900 (4)	92
D‡	10 mol % Y_2O_3 + 90 mol % ZrO_2	mixed oxide	1700 (15)	90
E‡	99 wt % (10 mol % Y_2O_3 + 90 mol % ZrO_2) + 1 wt % SiO_2	mixed oxide	1500 (15)	92
			1700 (15)	
F*	99 wt % (10 mol % Y_2O_3 + 90 mol % ZrO_2) + 1 wt % SiO_2	mixed oxide	1500 (15)	88

*Single crystal.
†Solution for coprecipitation prepared by dissolving zirconium carbonate (Magnesium Elektron Ltd) and Y_2O_3 in nitric acid.
‡ZrO_2 containing 2 wt % HfO_2 (Harshaw, > 99.5%), Y_2O_3 (Koch Light > 99.97%).

2. Experimental procedures

Single crystals of 8.7 mol % Y_2O_3 + 91.3 mol % ZrO_2 were obtained from W. & C. Spicers Ltd (St Mary's, Winchcomb, Gloucestershire). Specimens, 4 to 5 mm long for a.c. and 8 mm long for d.c. experiments with cross-sectional area 0.25 to 0.30 cm^2, were cut from irregularly shaped single crystals. These samples were polished on all six sides.

Most of the polycrystalline samples were prepared by thoroughly blending the oxide powders in water in the correct proportion using magnesia partially stabilized zirconia balls (Zircoa). Series B samples (Table I) were prepared by coprecipitation of the hydroxides by aqueous ammonia from a nitrate solution of zirconium and yttrium. The physically mixed or coprecipitated oxide powders were calcined, isostatically pressed into bar shapes at a pressure of 205 MN m^{-2} and sintered. Details of the sintering conditions and final densities are given in Table I. The polycrystalline samples were 20 to 25 mm long for d.c. and 4 to 6 mm long for complex impedance experiments and had a diameter between 5.5 and 6 mm.

Details of the 4 probe d.c. and complex impedance measurements have been described previously [17]. In summary, the four-probe d.c. data were recorded over the temperature range 400 to 1000° C at 25 to 50° C intervals for several heating and cooling cycles. The current values varied between 0.1 and 300 μA, depending upon the specimen resistance. The effect of time on the electrical conductivity was also studied at 1000° C. Normally it was small. For complex impedance experiments the temperature range was between 350 and 650° C and the data were recorded during a heating and a cooling cycle. A Solartron frequency response analyser 1174 interfaced with a DEC MINC 11/23 computer was used for a.c. measurements over the frequency range 1 to 10^6 Hz. Because of the overlap between the grain boundary and electrode arcs, a careful selection of the electrodes was sometimes necessary and on several occasions the experiments were repeated with a different electrode material. The electrodes used were: sputtered platinum, sputtered silver and electrodes made from a mixture consisting of 25 wt % PtO_2 and 75 wt % $(U_{0.38}Sc_{0.62})O_{2 \pm x}$ fluorite solid solution. The latter was used because of its low electrode resistance [18, 19].

3. Characterization

X-ray diffraction analysis of all the single crystal and polycrystalline samples showed the presence of a single fluorite phase. Single crystals were transparent and had a brownish colour which almost disappeared on extended annealing at 700° C in air. However, heat treatments of the single crystal specimens in the vicinity of 900 to 1000° C resulted in their turning opaque and white. X-ray analysis of these opaque samples again showed only a single fluorite phase. A partial disintegration and cracking was observed by optical microscopy. Similar behaviour was reported by Casselton [20] for Y_2O_3–ZrO_2 single crystals. Complex impedance data were collected on two transparent single crystals where the maximum temperature of the measurements was kept below 700° C, and on one opaque sample on which four-probe d.c. measurements had previously been made over the temperature range 400 to 1000° C (see below).

The reason for cracking of the single crystals is not clear and is peculiar to the W. & C. Spicers

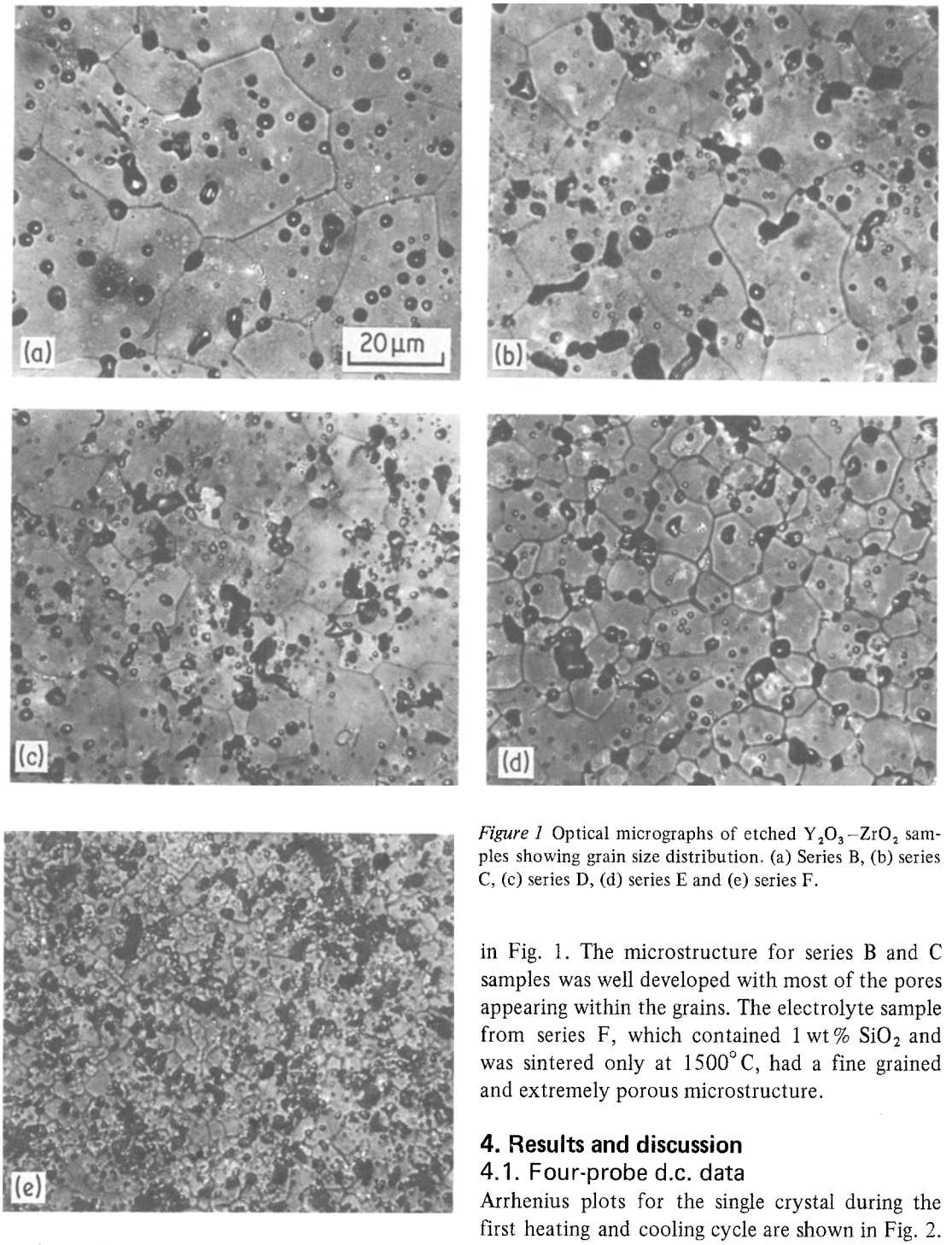

Figure 1 Optical micrographs of etched Y_2O_3–ZrO_2 samples showing grain size distribution. (a) Series B, (b) series C, (c) series D, (d) series E and (e) series F.

samples used in the present study. No such behaviour was observed for Y_2O_3–ZrO_2 single crystals prepared by Ceres Corporation, which remained transparent and clear on thermal cycling to 1000° C under identical conditions.

The optical micrographs of the various materials investigated, after suitable etching, are shown in Fig. 1. The microstructure for series B and C samples was well developed with most of the pores appearing within the grains. The electrolyte sample from series F, which contained 1 wt% SiO_2 and was sintered only at 1500° C, had a fine grained and extremely porous microstructure.

4. Results and discussion

4.1. Four-probe d.c. data

Arrhenius plots for the single crystal during the first heating and cooling cycle are shown in Fig. 2. The cooling data lay below those for heating, indicating a significant lowering of the conductivity. During subsequent cycling no further noticeable reduction in the conductivity was observed. The slopes of the Arrhenius plots were similar up to ~ 800° C. However, above 800° C the slope for the first heating cycle was much lower than that for

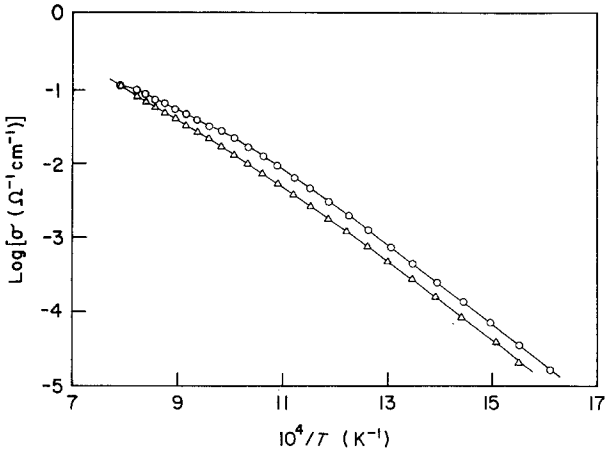

Figure 2 Arrhenius plots for the first heating (○) and cooling (△) cycle of the Y_2O_3–ZrO_2 single crystal.

the cooling cycle. In contrast, for polycrystalline samples the conductivities over the entire temperature range were identical for the first heating and the following cycles as shown in Fig. 3 for a typical sample. From these and previous observations it appears that the transparent single crystal began to crack above 800° C during the first heating cycle, resulting in a decrease in the conductivity. Since with increase in temperature the conductivity should increase, both processes combined to give an artificial slope in the temperature range 800 to 1000° C. The lower conductivity values thus obtained during the following thermal cycle are due to cracking and disintegration of the single crystal, consistent with the observations of the preceding section.

Arrhenius plots for the conductivity of representative polycrystalline samples are shown in Fig. 4 for a cooling cycle. For the sake of clarity the data for some samples have been omitted. The resistivities of various samples at several temperatures are given in Table II. Among polycrystalline samples, the maximum value of the conductivity was observed for the coprecipitated sample.

4.2. Complex impedance data

4.2.1. Polycrystalline samples

For polycrystalline materials two overlapping electrolyte arcs were observed in the complex impedance plane (Fig. 5). The arc on the right side in Fig. 5 is associated with grain boundaries and the arc on the left side is due to the lattice conductivity. The complex impedance data for two overlapping electrolyte arcs were analysed by a procedure similar to that described by Tsai and Whitmore [21], the details of which will be published elsewhere. The grain boundary relaxation was assumed to be in series with the lattice conductivity. A similar equivalent circuit has been proposed by Van Dijk and Burggraaf [22] for the brick-layer model.

Arrhenius plots for the volume and total conductivity of several samples are shown in Figs. 6 and 7. The grain boundary contributions, for

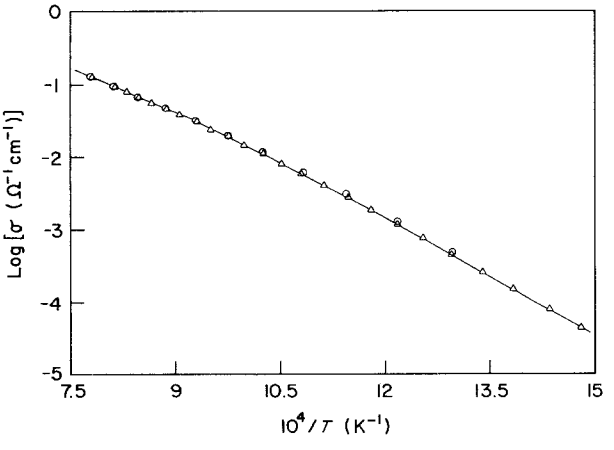

Figure 3 Arrhenius plots for the first heating (○) and cooling (△) cycle of a polycrystalline Y_2O_3–ZrO_2 sample.

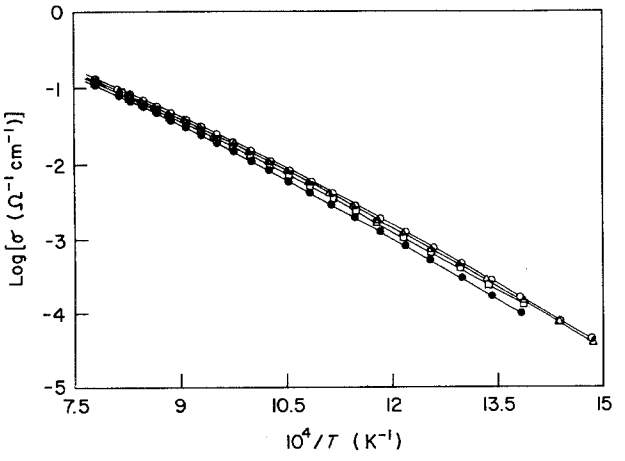

Figure 4 Arrhenius plots for the d.c. conductivity of various polycrystalline samples. ○, B1; △, C1; □, D1; ●, E1.

the sake of convenience and clarity also expressed as conductivities, are plotted in Fig. 8. The agreement between the four-probe d.c. data and the total conductivity as measured by the complex impedance technique was reasonably good. After separation of the grain boundary contribution, the volume conductivities of all the samples from series B to E were identical. The grain boundary resistance was relatively small in the purest polycrystalline samples and it increased from series B to D. During preparation of the samples for series C and D, Y_2O_3 and ZrO_2 powders were mixed zirconia) balls which contained impurities such as SiO_2 (~0.4 wt %). Thus minor impurity contamination is possible and it, in addition to the grain size effect obvious in Fig. 1, may also have contributed to the higher grain boundary resistance of these samples.

The greatest contribution to the grain boundary resistance was observed for samples form series E and F which contained deliberately added impurity (1 wt % SiO_2). Heat treatment of the samples from series F at 1700° C (series E) resulted in decreases in both the grain boundary and the volume resistance, although it was the grain boundary arc which was the more strongly affected (Fig. 5d and e). The minor increase in the volume conductivity is probably due to the increased density of sample E2 achieved by high-temperature sintering.

In general, the grain boundary resistance increased with decrease in the grain size and increase in the porosity (Figs. 1, 5 and 8). It also increased with impurity level and is more obvious in samples from series D and E both of which appear to have a similar grain size distribution but significantly different grain boundary resistance.

4.2.2. Single-crystal samples

Single crystal Y_2O_3–ZrO_2 samples gave one arc in the complex impedance plane, due to the lattice conductivity, over the entire temperature range (Fig. 9). However, below about 400° C the arc became slightly distorted on the low frequency side. The distortion was least for the transparent single crystal. A similar phenomenon is evident in

TABLE II D.C. resistivities of various samples at several temperatures

Sample	d.c. resistivity* (Ω cm)*					
	T(° C)					
	1000	800	700	600	500	450
A1†	–	25.1	57.1	208	1190	3615
A1	8.67	36.2	97.5	356	1975	5730
B1	8.41	32.3	93.8	351	2050	6530
C1	8.63	35.2	96.6	376	2195	6700
D1	9.04	38.0	105.7	405	2405	7415
E1	9.68	43.2	126.8	512	3230	10235

*Cooling cycle data except for A1†.
†First heating cycle data (transparent single crystal).

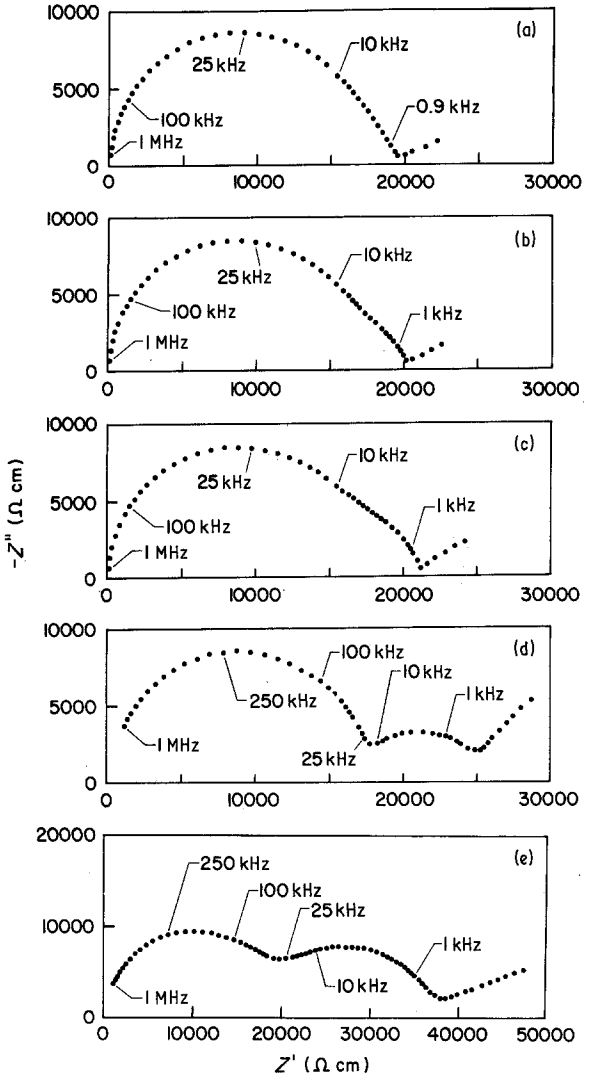

Figure 5 Complex impedance plane plots for the electrolyte behaviour of various samples at 400° C. (a) B2, (b) C2, (c) D2, (d) E2, and (e) F2. Note the different scale for (e).

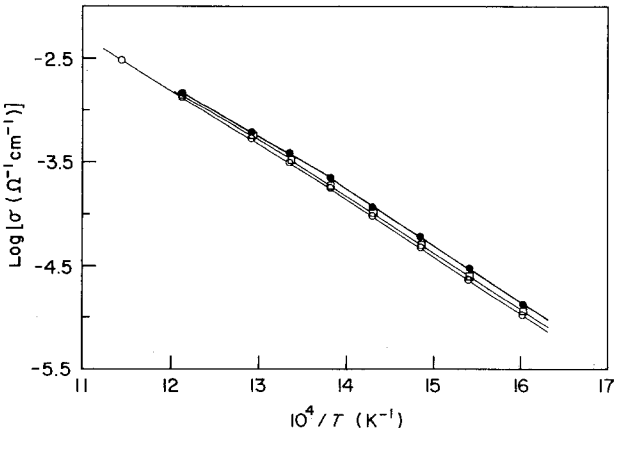

Figure 6 Temperature dependence of the volume (•, samples B2 and D2) and total a.c. (□, B2; ○, D2) conductivity.

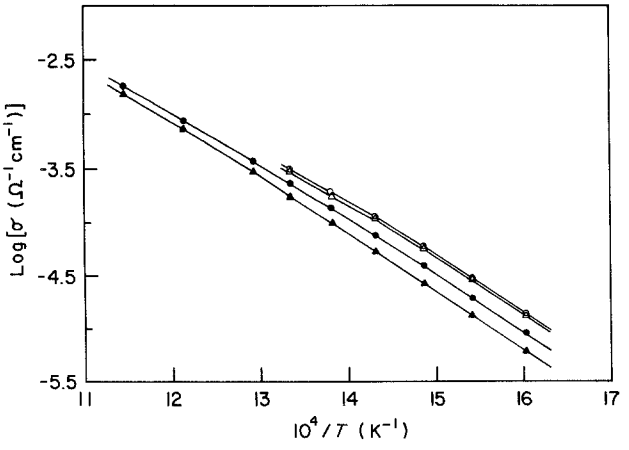

Figure 7 Temperature dependence of the volume (open symbols) and total (closed symbols) conductivity of samples E2 (○ ●) and F2 (△ ▲).

the work of Dragoo *et al.* (Fig. 4 in [14]). Our single crystals contained low-angle grain boundaries [23], which may have caused the minor distortion observed with transparent crystals. The greater distortion found with opaque crystals is attributed to internal cracking. All attemps to resolve the distorted arc into two arcs failed. Arrhenius plots for the a.c. conductivity of a transparent and the opaque single crystal are shown in Fig. 10. The electrical conductivity of the opaque sample, as expected, was lower than the transparent crystal. Again the impedance data for both the transparent and opaque crystals were in good agreement with the respective four-probe d.c. data.

4.3. Activation energy

The four-probe d.c. conductivity data of all samples including the single crystal showed a change in slope around 600° C towards a lower activation energy at higher temperatures. The activation energy for the high temperature region (850 to 1000° C) was 20 to 25 kJ mol^{-1} below that for the low temperature region (400 to 550° C) (Table III).

Activation energies for the total, volume and grain-boundary conductivities of various samples, as determined from the complex impedance data, are given in Table IV. The activation energy for the grain boundary conductivity was somewhat higher (5 to 10 kJ mol^{-1}) than that for the volume conductivity, consistent with the observations of Verkerk *et al.* [13]. Since the grain boundary conductivity is a complex phenomenon, no definite meaning can be assigned to the activation energy associated with the grain boundaries.

The values of activation energy for the total conductivity of transparent single crystals and the volume conductivity of polycrystalline samples were in the range 100 to 105 kJ mol^{-1}; similar to the values observed for the four-probe d.c. data in the same low temperature region but 20 to 25 kJ mol^{-1} higher than the four-probe d.c. values in the higher temperature range for both poly-

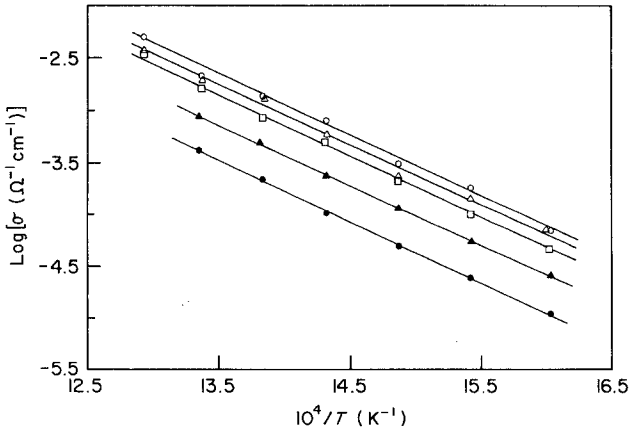

Figure 8 Arrhenius plots for the grain boundary conductivity of various samples. ○, B2; △, C2; □, D2; ▲, E2; ●, F2.

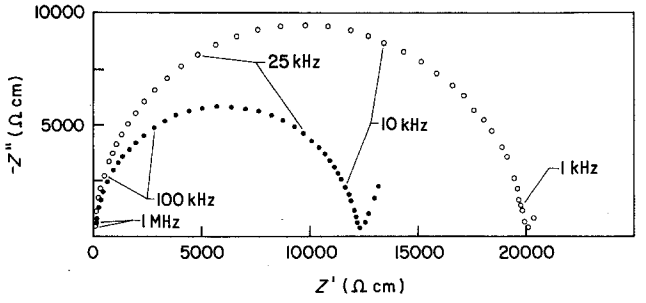

Figure 9 Complex impedance plane plots for the electrolyte behaviour of a transparent (•) and the opaque (○) single crystal samples at 400° C.

crystalline and single crystal samples. From these observations it can be concluded that the high activation energy observed in the low temperature region is associated with the lattice conductivity of the material. Comparable observations regarding the shape of the Arrhenius curves have been made by several authors on both polycrystalline and single-crystal Y_2O_3–ZrO_2 [7, 8, 13–15]. Thus there is considerable consensus between the literature and our own work that the change in the slope of the Arrhenius plots for the lattice conductivity of single crystals and pure polycrystalline samples is real and not an artefact of the measurement technique as suggested by Pascual *et al.* [16]. Another explanation must be sought.

For the lattice conductivity of ionic conductors as a function of temperature, Kilner and Waters [24] and Nowick and Park [25] have defined three stages or regions. Stage I occurs at very high temperatures where the conductivity is related to the intrinsic defects. Because of the high defect formation energies, the intrinsic defect concentration over most of the temperature range of interest is much less than the extrinsic concentration, and the contribution of this phenomenon to the conductivity can be ignored [6]. At low temperatures (stage III), dopant cations and vacancies form neutral defect pairs and the activation energy for conduction is a combination of the binding energy of the associates and the vacancy migration enthalpy. Stage II occurs in the intermediate temperature range and the conductivity in this region is determined by the concentration of charge-carrying defects which is controlled by the aliovalent dopant.

Wang *et al.* [26] demonstrated that dopant cation–vacancy complexes exist at low temperatures in CeO_2–Y_2O_3 solid solutions containing low concentrations of Y_2O_3. They also concluded that the effective activation enthalpy for conduction at low temperatures included contributions from the enthalpies of association and vacancy migration. Kilner and Steele [6], after reviewing the work of several authors, have found significant evidence for the occurrence of defect association effects, at low temperatures, in fluorite-type oxygen ion conductors. The interpretation of the conductivity data for higher concentrations of the dopant level (as certainly is the case in the present study) is difficult because of the complex nature of the vacancy–dopant cation interactions [26] and is further complicated by the ordering of vacancies

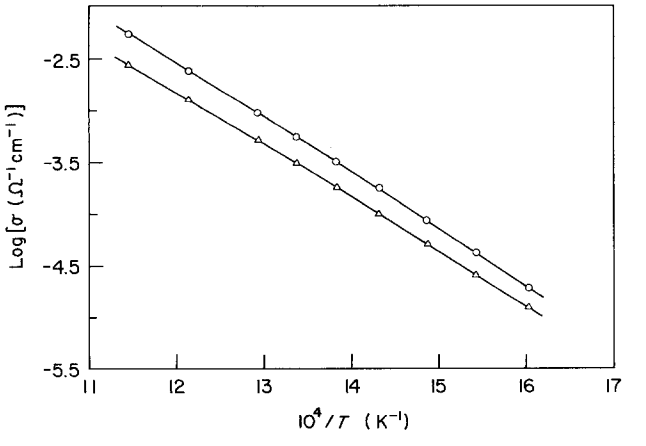

Figure 10 Arrhenius plot for the a.c. conductivity of a transparent (○) and opaque (△) single crystals.

TABLE III Activation energies for the high and low temperature regions from four-probe d.c. conductivity data

	E^* (kJ mol^{-1})	
	Temperature range 850–1000° C	Temperature range 400–500° C
A1	80 ± 2	101 ± 2
B1	78 ± 2	105 ± 2
C1	78 ± 2	105 ± 2
D1	80 ± 3	103 ± 2
E1	83 ± 2	108 ± 3
F1	83 ± 2	104 ± 3

*Average of several heating and cooling cycles.

TABLE IV Activation energy for the total, volume and grain-boundary conductivity (350 to 500° C)

Sample	E (kJ mol^{-1})		
	Total	Volume	Grain boundary
A1*	100 ± 3	97 ± 3	–
A2†	–	100 ± 2	–
A3†	–	105 ± 3	–
B2	106 ± 3	105 ± 3	109 ± 5
C2	104 ± 3	103 ± 3	109 ± 7
D2	106 ± 3	104 ± 3	113 ± 4
E2	103 ± 3	101 ± 5	109 ± 3
F2	105 ± 4	101 ± 4	111 ± 3

*Opaque single crystal.
†Transparent single crystals.

and cations (existence of microdomains etc.) [27, 28]. From the above discussion it appears that the higher activation energy observed below 600° C in our samples is related to the existence of vacancy–dopant cation complexes.

5. Conclusions

Both impurities and poorly defined electrolyte microstructures result in higher grain boundary resistance and can be detrimental to the performance of solid state devices at low temperatures. For example in commercial stabilized zirconia grain boundaries have been considered as the possible cause for e.m.f. drifts normally observed in oxygen sensors. This work clearly demonstrates that with appropriate purity of the materials and for well prepared solid electrolytes the grain boundary resistance can be significantly reduced. Careful analysis of the four-probe d.c. and complex impedance data also revealed that the Arrhenius plots of the conductivity show curvatures, the activation energy decreasing with increased temperature. This change in the slope is a property intrinsic to the lattice conductivity of the materials and is not related to an increased grain boundary contribution as temperature decreases. Sufficient evidence exists for the formation of dopant cation–vacancy associates at low temperatures and such an explanation for the change in activation energy appears to be more feasible and should be further investigated.

Acknowledgements

The author wishes to thank Mr F. T. Ciacchi, Mr R. K. Stringer and Miss B. Terrell for their assistance with the preparation of specimens. Many useful discussions with Drs M. J. Bannister and R. H. J. Hannink are greatly appreciated. The manuscript was kindly reviewed by Dr M. J. Bannister. Partial support for this project was provided under the National Energy Research Development and Demonstration Program which is administered by the Commonwealth Department of National Development and Energy of Australia.

References

1. T. H. ETSELL and S. N. FLENGAS, *Chem. Rev.* **70** (1970) 339.
2. D. YUAN and F. A. KRÖGER, *J. Electrochem. Soc.* **116** (1969) 594.
3. H. OBAYASHI and T. KUDO, in "Solid State Chemistry of Energy Conversion and Storage", Advances in Chemistry Series, Vol. 163, edited by J. B. Goodenough and M. S. Whittingham (The American Chemical Society, Washington, D.C., 1977) p. 316.
4. N. M. BEEKMANS and L. HEYNE, *Electrochim. Acta* **21** (1976) 303.
5. M. KLEITZ, H. BERNARD, E. FERNANDEZ and E. SHOULER, in "Advances in Ceramics", Vol. 3, edited by A. H. Heuer and L. W. Hobbs (The American Ceramic Society, Columbus, Ohio, 1981) p. 310.
6. J. A. KILNER and B. C. H. STEELE, in "Non-stoichiometric Oxides", edited by O. T. Sørensen (Academic Press, London, 1981) p. 233.
7. E. SCHOULER, PhD thesis, Grenoble, France (1980).
8. J. E. BAUERLE and J. HRIZO, *J. Phys. Chem. Solids* **30** (1969) 565.
9. M. V. INOZEMTSEV and M. V. PERFIL'EV, *Elektrokhimiya* **11** (1975) 1031.
10. M. J. VERKERK, A. J. A. WINNUBST and A. J. BURGGRAAF, *J. Mater. Sci.* **17** (1982) 3113.
11. M. V. INOZEMTSEV, M. V. PERFIL'EV and A. S. LIPILIN, *Elektrokhimiya* **10** (1974) 1471.
12. A. I. IOFFE, M. V. INOZEMTSEV, A. S. LIPILIN, M. V. PERFIL'EV and S. V KARPACHOV, *Phys. Status Solidi (a)* **30** (1975) 87.
13. M. J. VERKERK, B. J. MIDDLEHUIS and A. J.

BURGGRAAF, *Solid State Ionics* **6** (1982) 159.
14. A. L. DRAGOO, C. K. CHIANG and A. D. FRANKLIN, *ibid.* 7 (1982) 249.
15. P. ABELARD and J. F. BAUMARD, *Phys. Rev. B* **26** (1982) 1005.
16. C. PASCUAL, J. R. JURADO and P. DURAN, *J. Mater. Sci.* **18** (1983) 1315.
17. S. P. S. BADWAL, *J. Mater. Sci.* **18** (1983) 3117.
18. *Idem, J. Electroanal. Chem.* in press.
19. S. P. S. BADWAL, M. J. BANNISTER and W. G. GARRETT, Proceedings of the Second Zirconia Technologies Conference, Stuttgart, 21–23 June 1983, edited by A. H. Heuer, N. Clausser and M. Ruble (The American Ceramic Society, Columbus, Ohio, 1984).
20. R. E. W. CASSELTON, *Phys. Status Solidi (a)* **2** (1970) 571.
21. Y.-T. TSAI and D. H. WHITMORE, *Solid State Ionics* 7 (1982) 129.
22. T. VAN DIJK and A. J. BURGGRAAF, *Phys. Status Solidi (a)* **63** (1981) 229.
23. R. H. J. HANNINK, private communication (1983).
24. J. A. KILNER and C. D. WATERS, *Solid State Ionics* **6** (1982) 253.
25. A. S. NOWICK and D. S. PARK, in "Superionic Conductors", edited by G. Mahen and W. Roth (Plenum Press, New York, 1976) p. 395.
26. DA YU WANG, D. S. PARK, J. GRIFFITH and A. S. NOWICK, *Solid State Ionics* **2** (1981) 95.
27. R. E. CARTER and W. L. ROTH, in "Electromotive Force Measurements in High Temperature Systems", edited by C. B. Alcock (Elsevier, Amsterdam, 1968) p. 125.
28. H. J. ROSSELL, in "Advances in Ceramics", Vol. 3, edited by A. H. Heuer and L. W. Hobbs (The American Ceramic Society, Columbus, Ohio, 1981) p. 47.

Received 8 August
and accepted 13 September 1983